Ⅵ Figures and Legends

Figure 1. Diagrammatic representation of the development of the eye in a generalized vertebrate.

A: Five brain vesicles and spinal cord. The optic vesicles evaginate from the wall of the diencephalon. **B:** The development of the eye. The optic vesicle invaginates to form a double-layered optic cup. The lens placode is made from the overlying ectoderm. The optic cup develops the neural retina and pigmented epithelium as the lens is internalized.

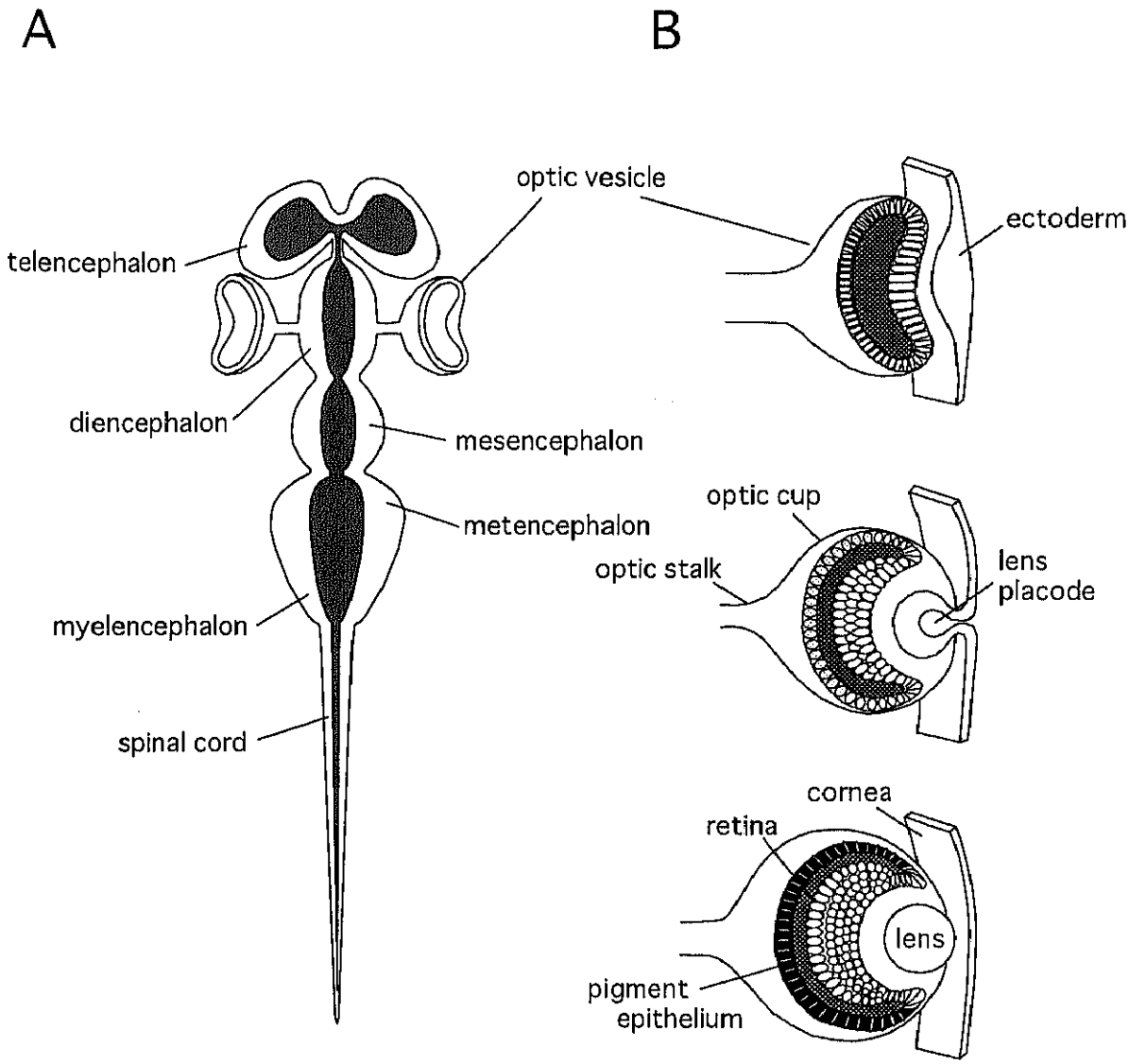
A
B
optic vesicle
telencephalon
diencephalon
mesencephalon
metencephalon
myelencephalon
spinal cord
ectoderm
optic cup
optic stalk
lens
placode
cornea
retina
lens
pigment
epithelium

Figure 2. Schematic diagram showing typical retinal neurons of the vertebrate retina and organization of retinal layers.

R, rod photoreceptor cell; C, cone photoreceptor cell; H, horizontal cell; B, bipolar cell; A, amacrine cell; G, ganglion cell; M, Müllar cell; PCL, pigment cell layer; RCL, receptor cell layer; ONL, outer nuclear layer; OPL, outer plexiform layer; INL, inner nuclear layer; IPL, inner plexiform layer; GCL, ganglion cell layer.

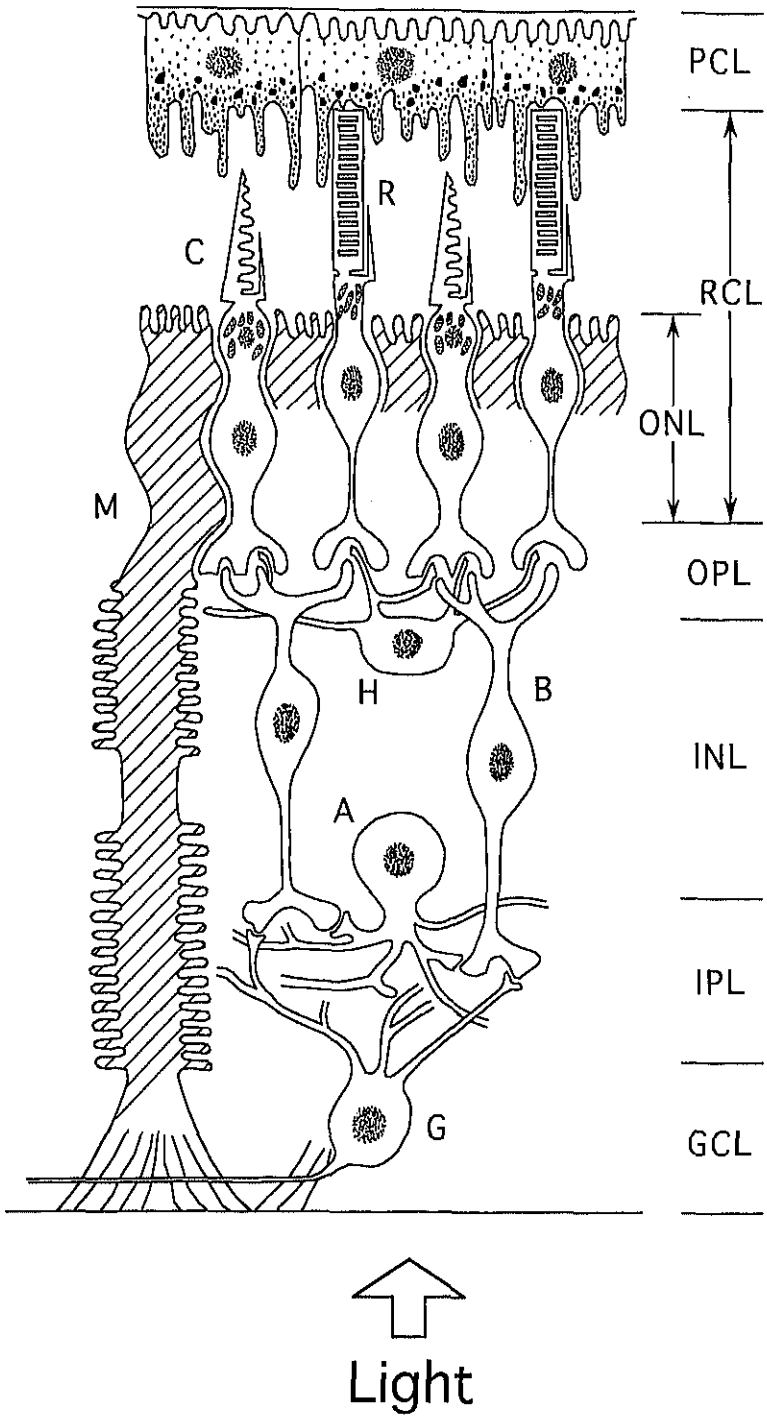
PCL
R
C
RCL
ONL
M
OPL
H
B
INL
A
IPL
G
GCL
Light

Figure 3. Schematic diagram showing intracellular communication in a chemical and an electrical synapse.

A: Chemical synapse. Chemical synapses can be divided into excitatory and inhibitory synapses by the nature of the postsynaptic response. At the chemical synapse, neuronal signals are transmitted by neurotransmitters. Typical excitatory neurotransmitters are L-glutamate and acetylcholine, and inhibitory neurotransmitters are GABA and glycine. The neurotransmitter is stored in synaptic vesicles located in the presynaptic terminal and released by exocytosis in response to its depolarization. When the neurotransmitters diffuse across the synaptic cleft and bind to their specific receptors, a depolarizing potential is elicited in the postsynaptic cell at excitatory synapse, while at inhibitory synapse, a hyperpolarizing potential is generated. **B:** Electrical synapse. Some ions and a certain small molecules can pass directly through a specific kind of intercellular contact called gap junction.

A

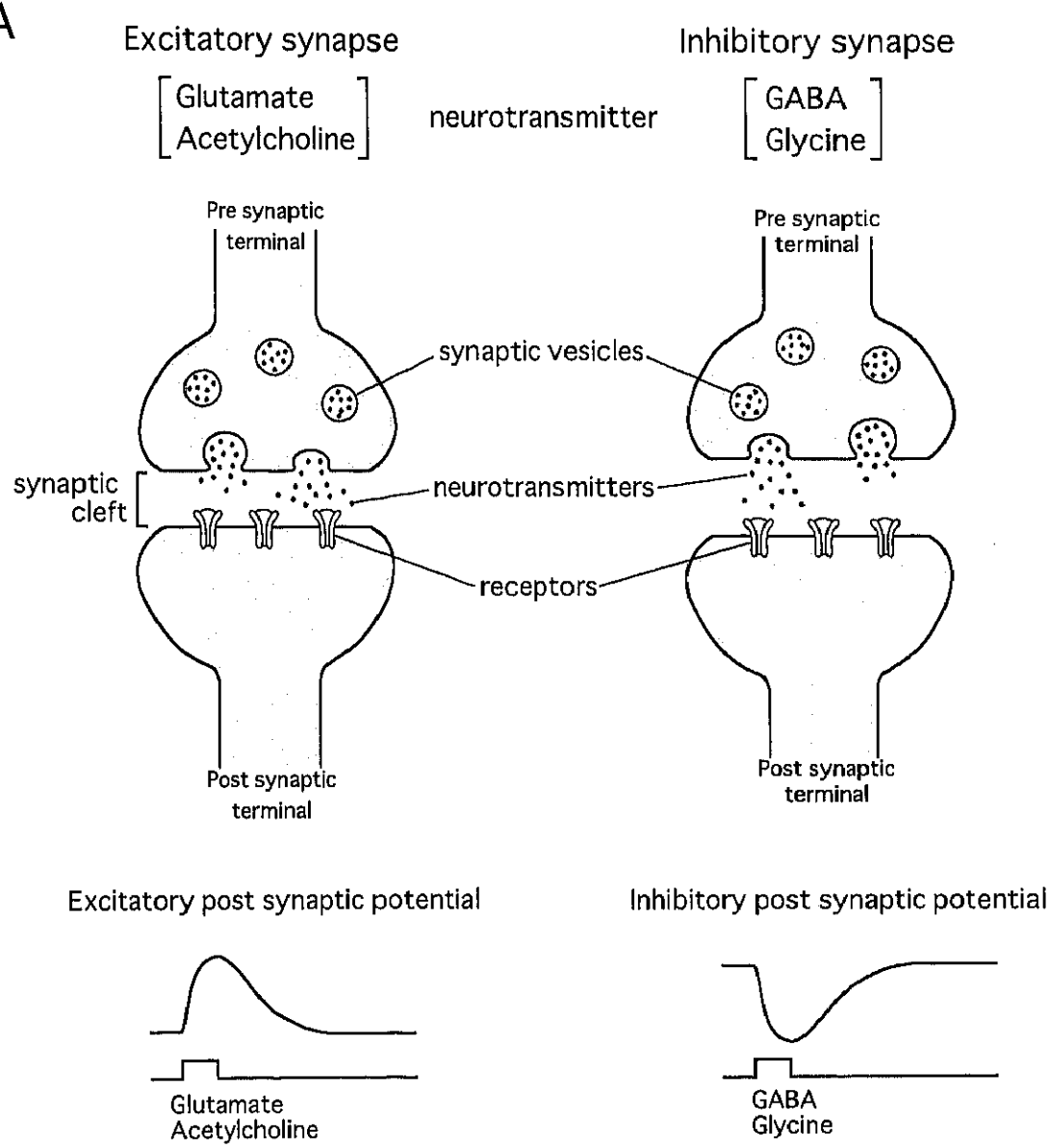
Excitatory synapse
Glutamate
Acetylcholine
neurotransmitter
Inhibitory synapse
GABA
Glycine
Pre synaptic terminal
Pre synaptic terminal
synaptic vesicles
synaptic cleft
neurotransmitters
receptors
Post synaptic terminal
Post synaptic terminal
Excitatory post synaptic potential
Glutamate
Acetylcholine
Inhibitory post synaptic potential
GABA
Glycine

B

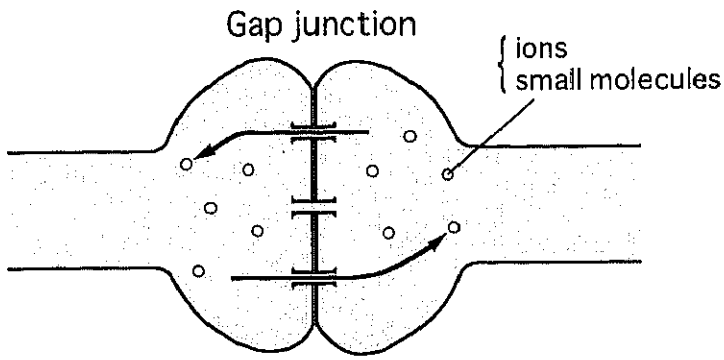
Gap junction
ions
small molecules

Figure 4. Outline of operative procedures to surgical removal of the normal retina from the adult newt eye.

After a deeply anesthetized animal was placed on a chamber (**A**), the dorsal half of the eye was cut open along the cornea-scleral junction (**B**). The retina and lens were removed (**C**), and then the eye flap consisting of iris and cornea was gently replaced at its original position (**D**). The other eye was left intact as a control.

A

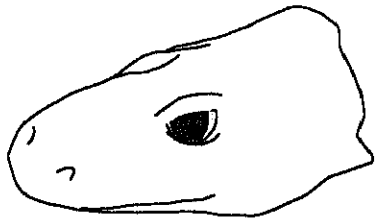

B

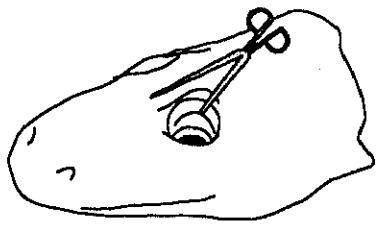

C

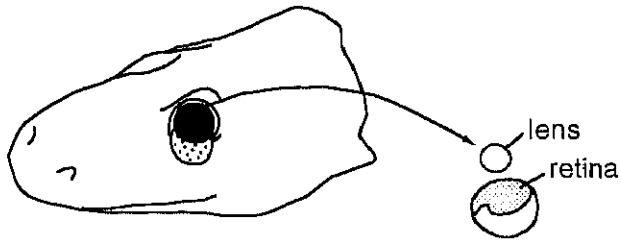

D

Figure 5. Outline of procedures for making the living slice preparations. An eyeball is cut open into four sectors from above (**A**). The lens is removed to expose the retina (**B**). After the retina is wetted with a newt saline solution containing 0.1% bovine serum albumin, another filter paper is mounted on it (**C**). Following removal of the sclera and choroid, the retina adhering to the mounted filter paper (**D**) is sliced transretinally together with the filter paper with a McIlwain tissue chopper (**E**). Sliced retinas are set on a chamber for whole-cell patch-clamp recording (**F**). The chamber is mounted on uplight microscope stage. Experimental solutions are continuously supplied by gravity through an inlet tube (*inlet*) and aspirated away through an outlet tube (*outlet*). A reference electrode is connected to the experimental solutions via 3 M KCl agar bridge. The patch electrode is filled with a solution including biocytin and Lucifer Yellow, together with ions designed to carry the currents of interest but not others. Whole-cell current detected by the patch electrode is amplified by a patch-clamp amplifier (*OA*). Current data are stored in a computer hard disk for off-line analysis and presentation.

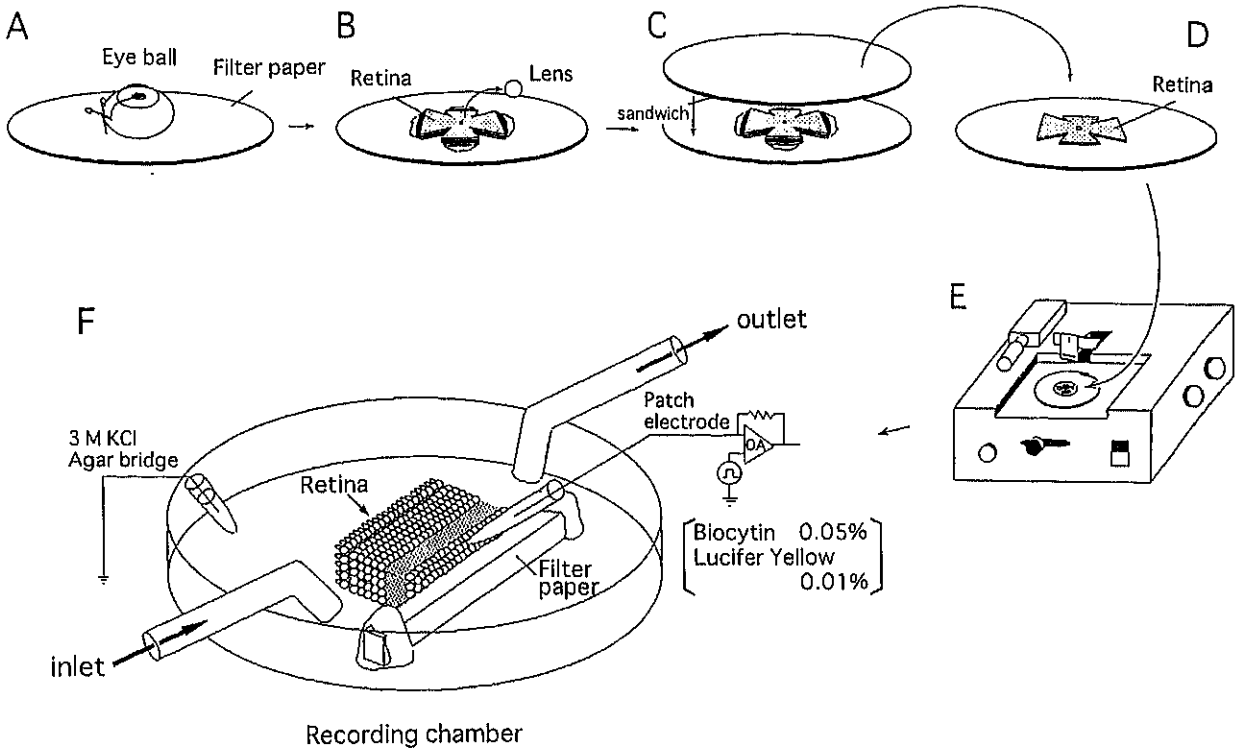
A
Eye ball
Filter paper
B
Retina
Lens
C
sandwich
D
Retina
E
F
outlet
Patch
electrode
OA
3 M KCl
Agar bridge
Retina
Filter
paper
Biocytin 0.05%
Lucifer Yellow
0.01%
inlet
Recording chamber

Figure 6. Cellular structure of the adult newt retina.

A: Photomicrograph of a living slice preparation of adult newt retina under Nomarski optics. **B:** Schematic diagram showing the structure of the newt retina. This drawing is based on the result obtained from intracellular staining experiment (Umino et al. 2003). R, receptor cell; H, horizontal cell; B, bipolar cell; A, amacrine cell; G, ganglion cell; PCL, pigment cell layer; RCL; receptor cell layer; OPL, outer plexiform layer; INL, inner nuclear layer; IPL, inner plexiform layer; GCL, ganglion cell layer; filter, filter paper. Scale bar = 60 μm.

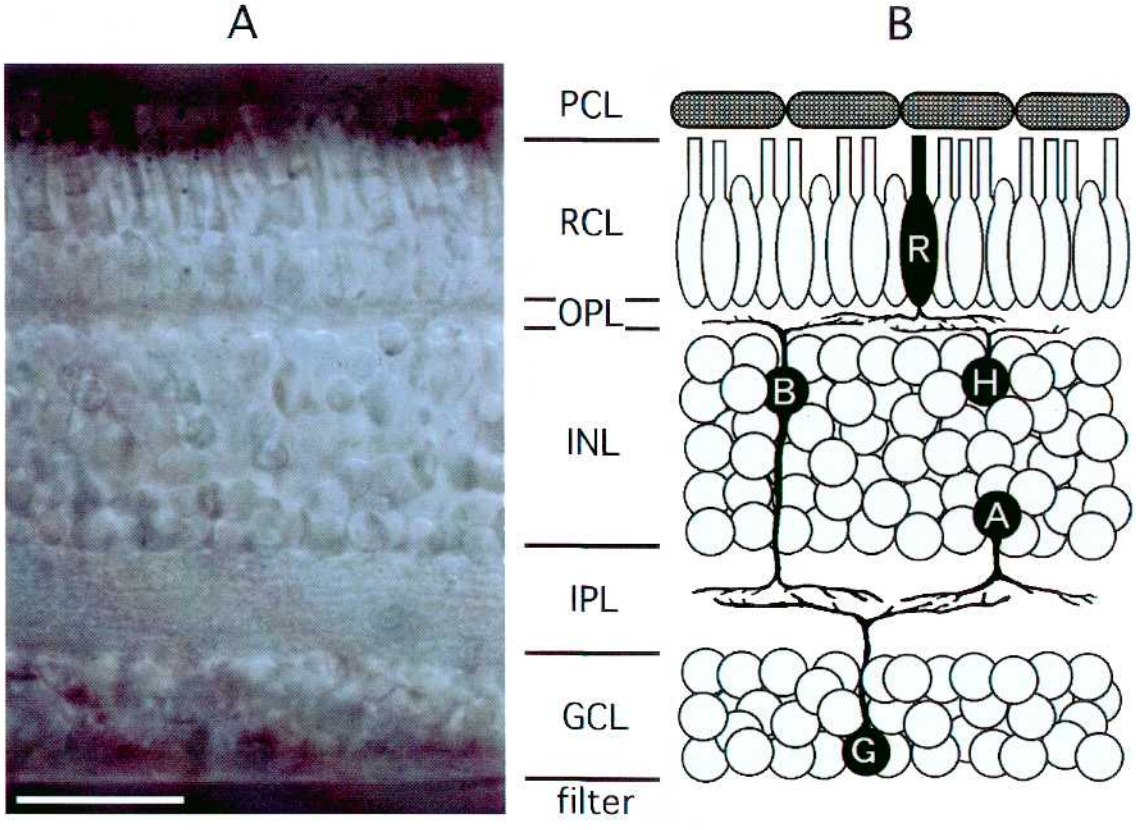
A
B
PCL
RCL
OPL
INL
IPL
GCL
filter
R
B
H
A
G

Figure 7. Procedures for morphological identification of biocytin-injected cells.

Iontophoretical injection of biocytin (0.5 mg/ml) into current recorded cell in sliced retina (400 µm thickness) (-1 nA, 100 Hz, for 10 min)

↓

Fixation in 4% paraformaldehyde in 0.1 M PB at pH 7.4 (12h/ 4℃)

↓

Washing in 0.02 M PBS (15 min)

↓

Incubation in the Avidin Biotin peroxidase Complex (ABC-Elite, Vector Labs) (3-5 days in dark/ 4℃)

↓

Washing in PBS (three times/ 15 min each)

↓

Incubation in diaminobenzidine (DAB substrate kit) to visualized the recorded cells (4-10 min/ RT)

↓

Termination of the DAB reaction of biocytin by immersing the tissue in PBS

↓

Examination under light microscope

Figure 8. Slice preparation of regenerating retinas corresponding to five progressive stages (**A**) and a schematic diagram showing morphological characteristics of retinas at each regenerating stage (**B**).

In **A**, a dotted arrow indicates the presumptive IPL. F, filter paper; RCL, receptor cell layer; OPL, outer plexiform layer; INL, inner nuclear layer; IPL, inner plexiform layer; GCL, ganglion cell layer. Scale bar = 20 μm.

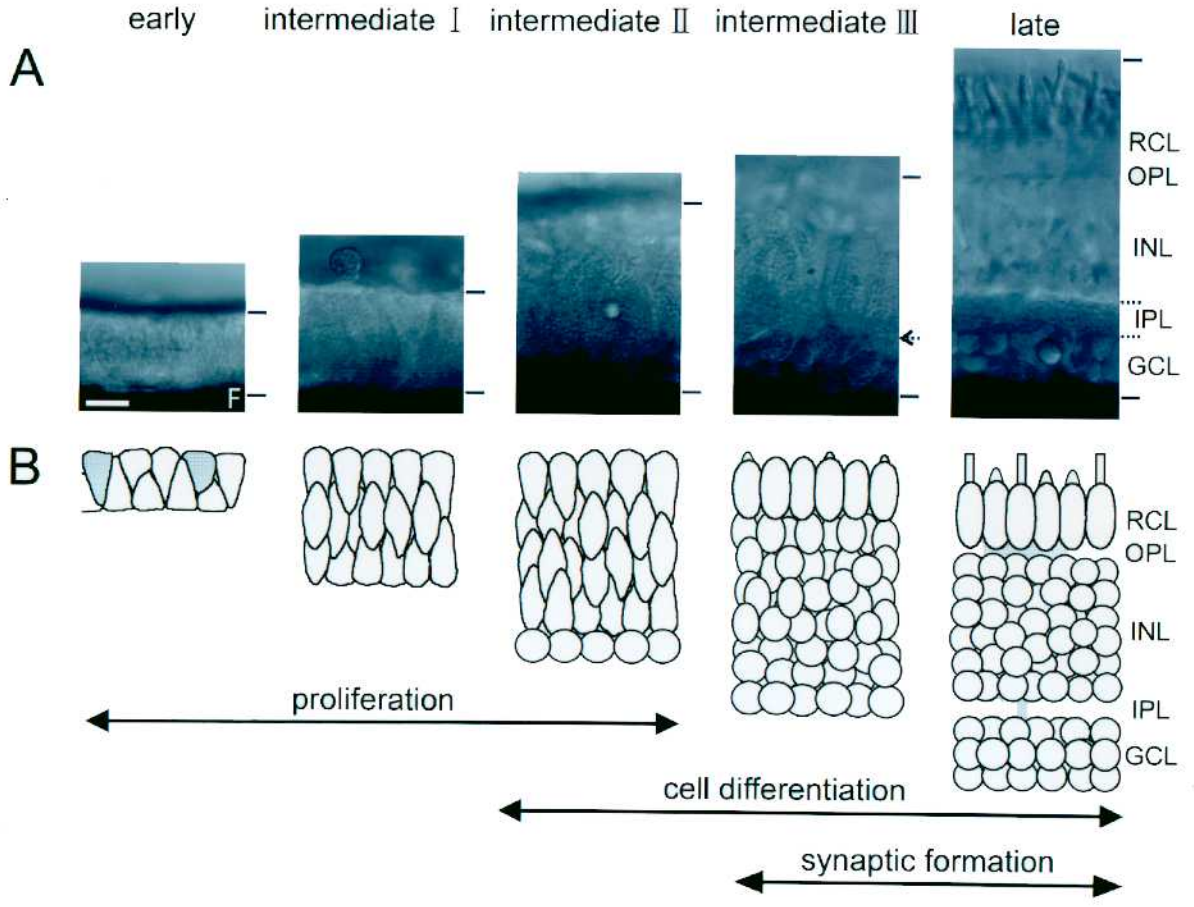
early
intermediate Ⅰ
intermediate Ⅱ
intermediate Ⅲ
late
A
RCL
OPL
INL
IPL
GCL
F
B
RCL
OPL
INL
IPL
GCL
proliferation
cell differentiation
synaptic formation

Figure 9. Whole-cell currents of a progenitor cell and tracer coupling with its neighbors in the 'intermediate-I' regenerating retina.

Cell was injected with both LY and biocytin after current recordings. **A:** Cell was initially voltage-clamped at a holding potential of –80 mV close to the resting potential and then the membrane potential was stepped from –160 to 0 mV in 10 mV increments (inset). Step pulses of 525 ms duration were applied every 1 s. Currents were recorded while suppressing nonjunctional currents flowing through K^+ and Ca^{2+} channels. **B:** Current-voltage relationships (I-V curve), measured at 25 ms (**A**, arrow), of an intact progenitor cell (●) and a mechanically isolated solitary progenitor cell (○). **C:** Fluorescence micrograph of an LY-labeled cell. **D:** Light micrograph of tracer-coupled cells visualized with a DAB reaction of biocytin. F, Filter paper. Scale bar = 40 μm.

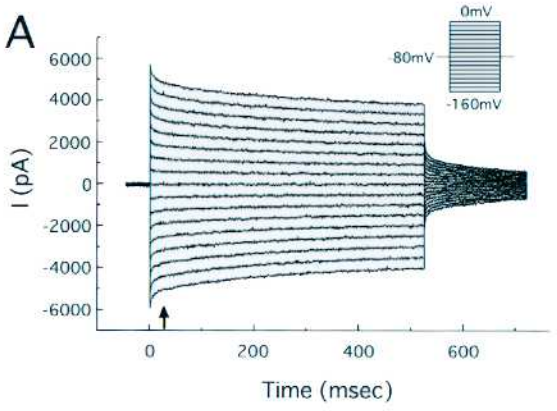
A
0mV
80mV
-160mV
6000
4000
2000
0
-2000
-4000
-6000
I (pA)
0
200
400
600
Time (msec)

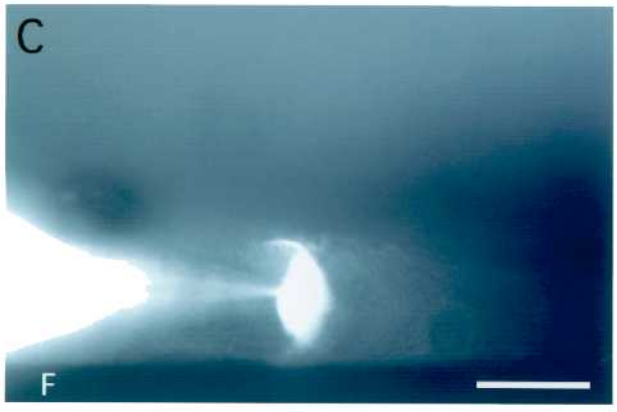
C
F

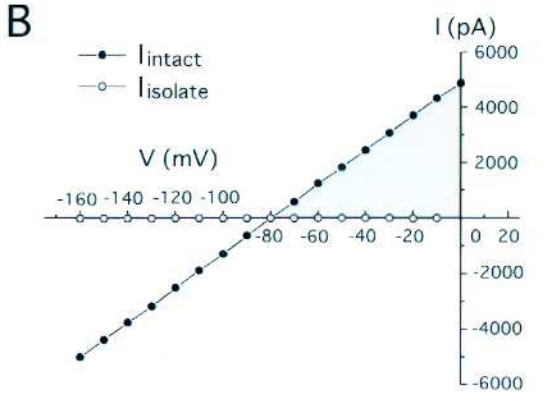
B
I (pA)
I intact
I isolate
V (mV)
-160 -140 -120 -100
-80 -60 -40 -20
0 20
6000
4000
2000
-2000
-4000
-6000

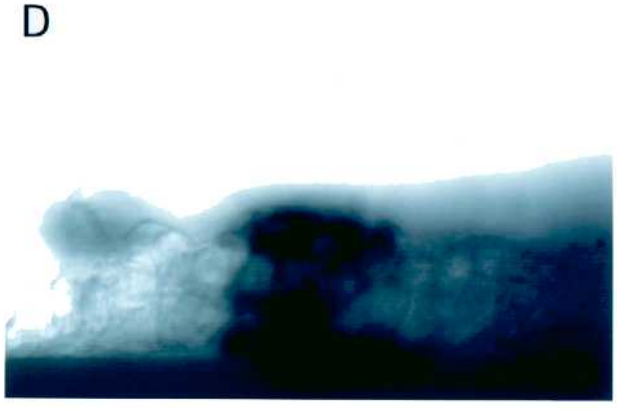
D

Figure 10. Time- and voltage-dependent decline of whole-cell currents of a progenitor cell and tracer coupling with its neighbors in the 'intermediate-I' regenerating retina.

Cell was injected with both LY and biocytin after current recordings. **A:** Cell was initially voltage-clamped at a holding potential of –66 mV close to the resting potential and then the membrane potential was stepped from –146 to +4 mV in 10 mV increments (inset). Other recording conditions are the same as those in Fig. 9A. **B:** The instantaneous (I_{inst}) and steady state (I_{ss}) currents, measured at 25 ms (●) and 524 ms (○) of each pulse, were plotted against the test voltage (V). **C:** Fluorescence micrograph of an LY-labeled cell in a slice preparation which was visualized under a combination of epifluorescent and incandescent lights. **D:** Light micrograph of tracer-coupled cells visualized with a DAB reaction of biocytin. F, filter paper. Scale bar = 40 μm.

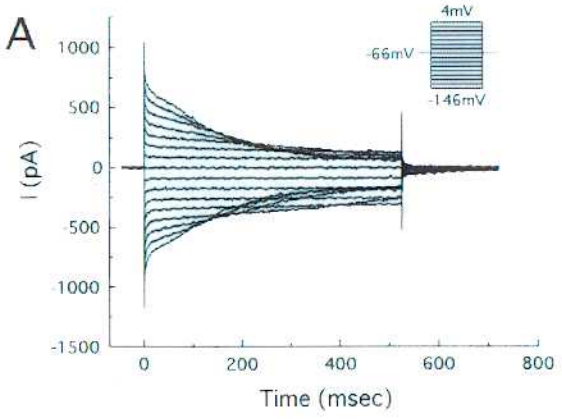
A
4mV
-66mV
-146mV
1000
500
0
-500
-1000
-1500
I (pA)
0
200
400
600
800
Time (msec)

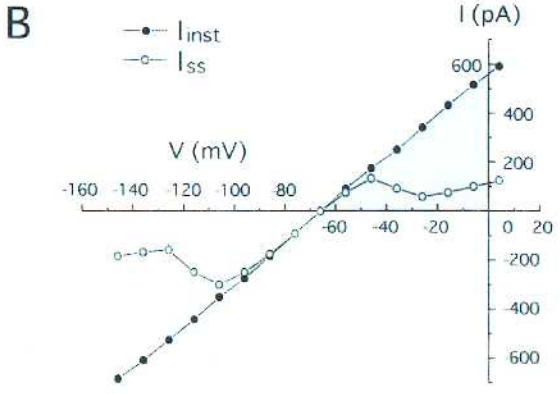
B
I (pA)
Iinst
Iss
600
400
200
V (mV)
-160
-140
-120
-100
-80
-60
-40
-20
0
20
-200
-400
600

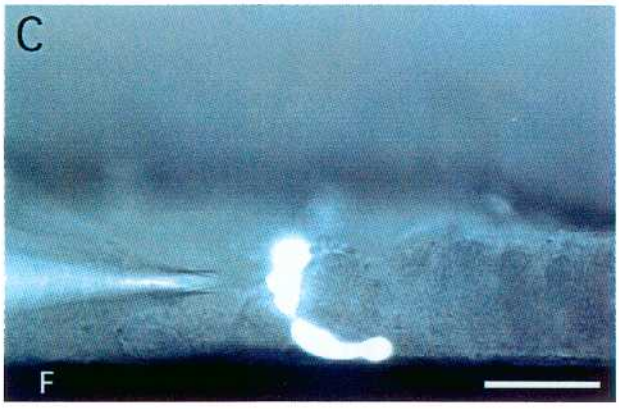
C
F

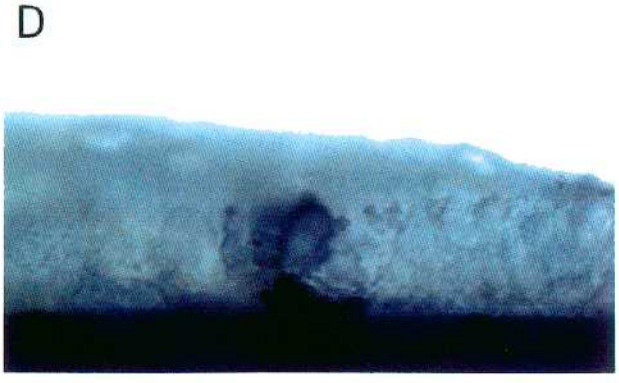
D

Figure 11. Effect of uncoupling agents on the whole-cell currents.

A: Effect of 18β-glycyrrhetinic acid (18β-GA). Cell was initially voltage-clamped at a resting potential of –80 mV and then the membrane potential was stepped from –180 to +20 mV in 50 mV increments. Left, whole-cell currents in the control solution. Voltage-clamped values are shown on the right of each current trace; Middle, currents at 30 s after application of 10 μM 18β-GA; Right, recovery of currents after 4 min of washing with 18β-GA -free solution.

B: Effect of octanol. Cell was initially voltage-clamped at a resting potential of –72 mV and then the membrane potential was stepped from –172 to +28 mV in 50 mV increments. Left, whole-cell currents in the control solution. Voltage-clamped values are shown on the right of each current trace; Middle, currents at 30 s after application of 500 μM octanol; Right, recovery of currents after 4 min of washing with octanol-free solution.

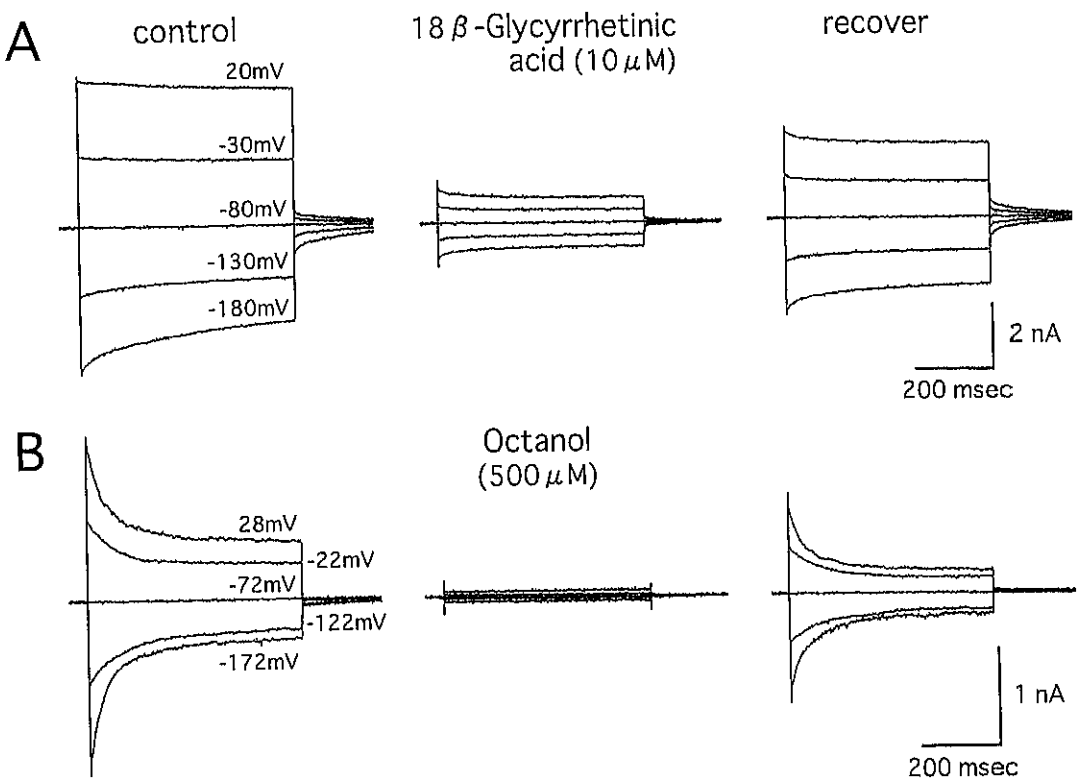
A
control
18 β-Glycyrrhetinic acid (10 μM)
recover
20mV
-30mV
-80mV
-130mV
-180mV
2 nA
200 msec
B
Octanol (500 μM)
28mV
-22mV
-72mV
-122mV
-172mV
1 nA
200 msec

Figure 12. Time- and voltage-dependent decline of whole-cell currents of a progenitor cell and tracer coupling with its neighbors in the 'intermediate-II' regenerating retina.

A: Cell was initially voltage-clamped at a holding potential of –63 mV and then the membrane potential was stepped from –143 to +17 mV in 10 mV increments (inset). Other recording conditions are the same as those in Fig. 9A. **B:** Fluorescence micrograph of an LY-labeled cell with a slender shape as shown in **A**. **C:** Light micrograph of tracer-coupled cells (arrow) visualized with a DAB reaction of biocytin. **D:** A horizontal section of the slice retina shown in **C**. An arrow indicates a cluster of biocytin-labeled cell. F, filter paper. Scale bar = 40 μm.

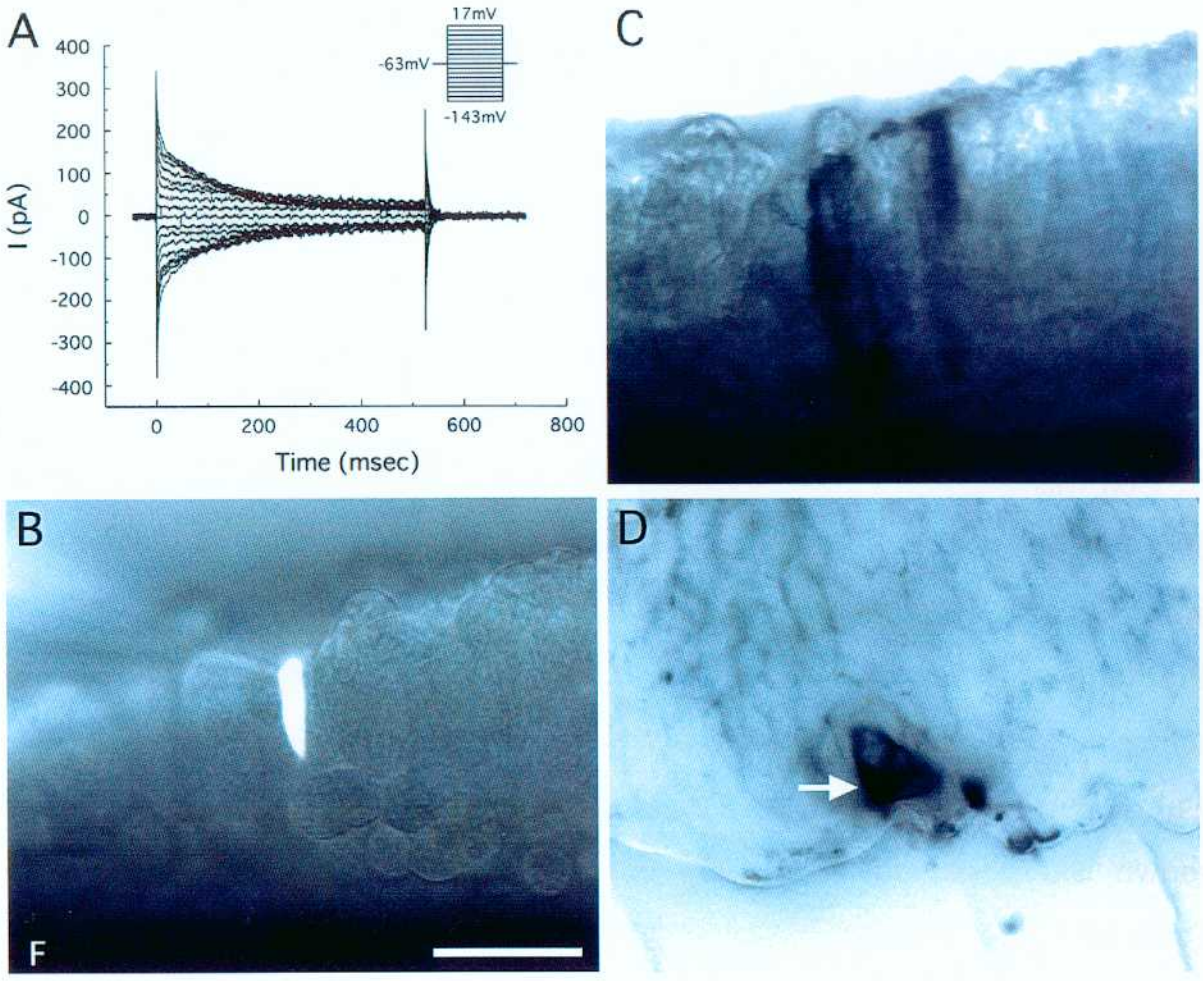
A
17mV
-63mV
-143mV
400
300
200
100
0
-100
-200
-300
-400
I (pA)
0
200
400
600
800
Time (msec)
C
B
F
D

Figure 13. Whole cell currents and morphology of a presumed premature ganglion cell in the 'intermediate-II' regenerating retina.

A: Cell was initially voltage-clamped at a holding potential of –18 mV close to the resting potential and then the membrane potential was stepped from –98 to +62 mV in 10 mV increments (inset). Other recording conditions are the same as those in Fig. 9A. **B:** The same cell was voltage-clamped at a holding potential of –100 mV and then the membrane potential was stepped from –120 to +50 mV in 10 mV increments. Each step pulse of 8 ms duration was applied every 1 s. Capacitive and leakage currents were reduced by subtraction program as described in the Methods. **C:** Fluorescence micrograph of an LY-labeled cell recorded above with a round soma localized at the most proximal level of the retina. This slice preparation was visualized under a combination of epifluorescent and incandescent lights. **D:** Light micrograph of the biocytin-labeled cell as shown above. No tracer coupling was observed. F, filter paper. Scale bar = 40 μm.

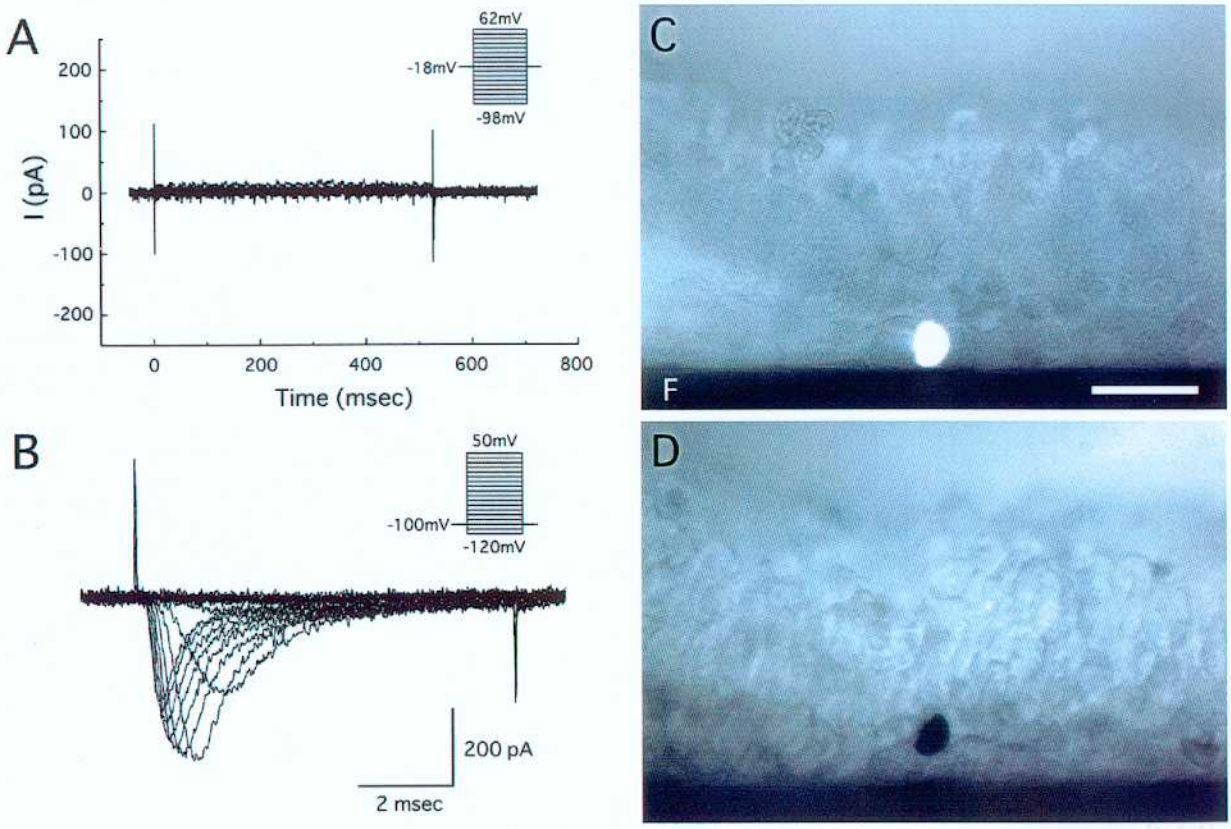
A
62mV
-18mV
-98mV
200
100
0
-100
-200
I (pA)
0
200
400
600
800
Time (msec)
B
50mV
-100mV
-120mV
200 pA
2 msec
C
F
D

Figure 14. Whole-cell currents of a progenitor cell and tracer coupling with its neighbors in the ciliary marginal zone (CMZ) of the 'intermediate-III' regenerating retina.

A: Cell was initially voltage-clamped at a holding potential of –63 mV, and then the membrane potential was stepped from –143 to +17 mV in 10 mV increments (inset). Other recording conditions are the same as those in Fig. 9A. **B:** Fluorescence micrograph of an LY-labeled cell. This slice preparation was visualized under a combination of epifluorescent and incandescent lights. **C:** Light micrograph of tracer-coupled cells visualized by incubation of the biocytin-filled cells in DAB. An asterisk indicates the LY-injected cell. **D:** Drawing of the outline of the retina and tracer-coupled area (gray screen). An asterisk indicates the LY-injected cell. P, pigment epithelium. F, filter paper. Scale bar = 40 μm.

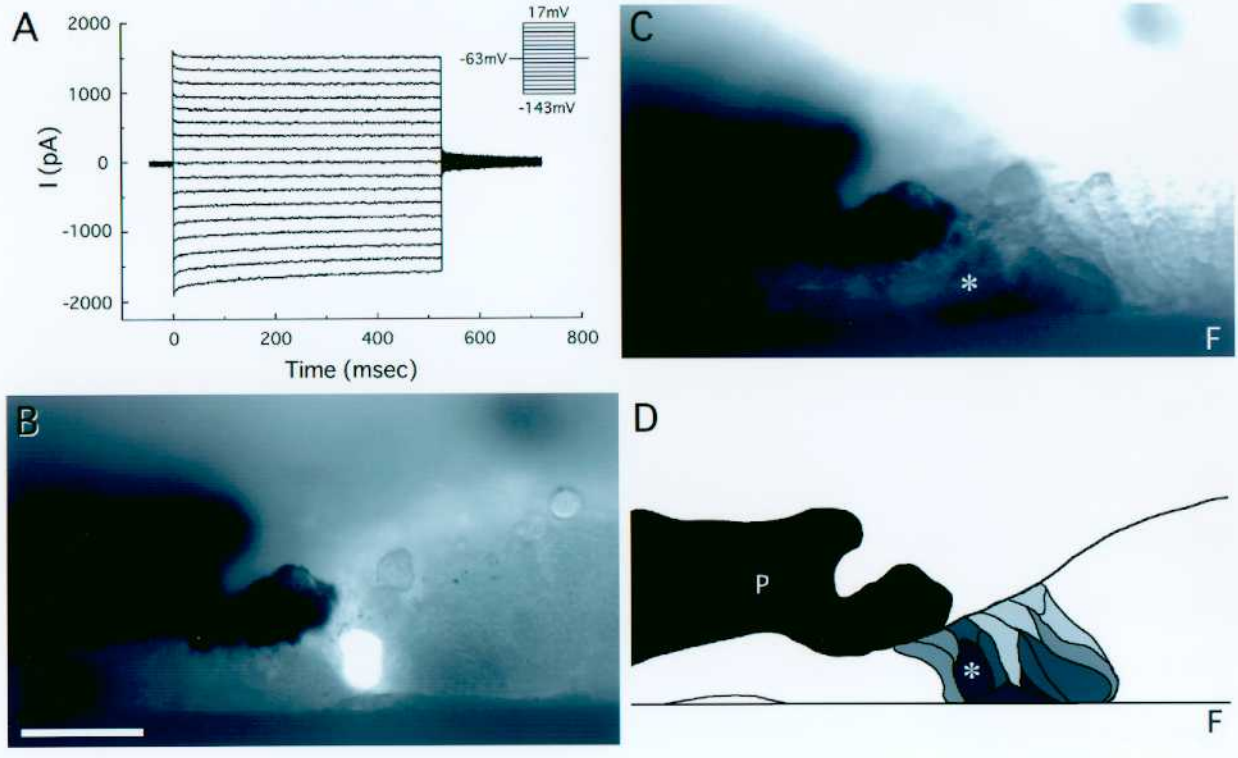
A
2000
1000
0
-1000
-2000
I (pA)
0
200
400
600
800
Time (msec)
17mV
-63mV
-143mV
B
C
*
F
D
P
*
F

Figure 15. Tracer coupling of ganglion cells in a control retina.

Both LY and biocytin were injected into a single cell after current recordings. **A:** Fluorescence micrograph of an LY-labeled cell. This slice preparation was visualized under a combination of epifluorescent and incandescent lights. **B:** Tracer coupled cells are indicated by arrowheads. A LY-injected cell (asterisk) was detached after the DAB reaction procedures. Abbreviations are the same as those in Fig. 8. Scale bar = 40 μm.

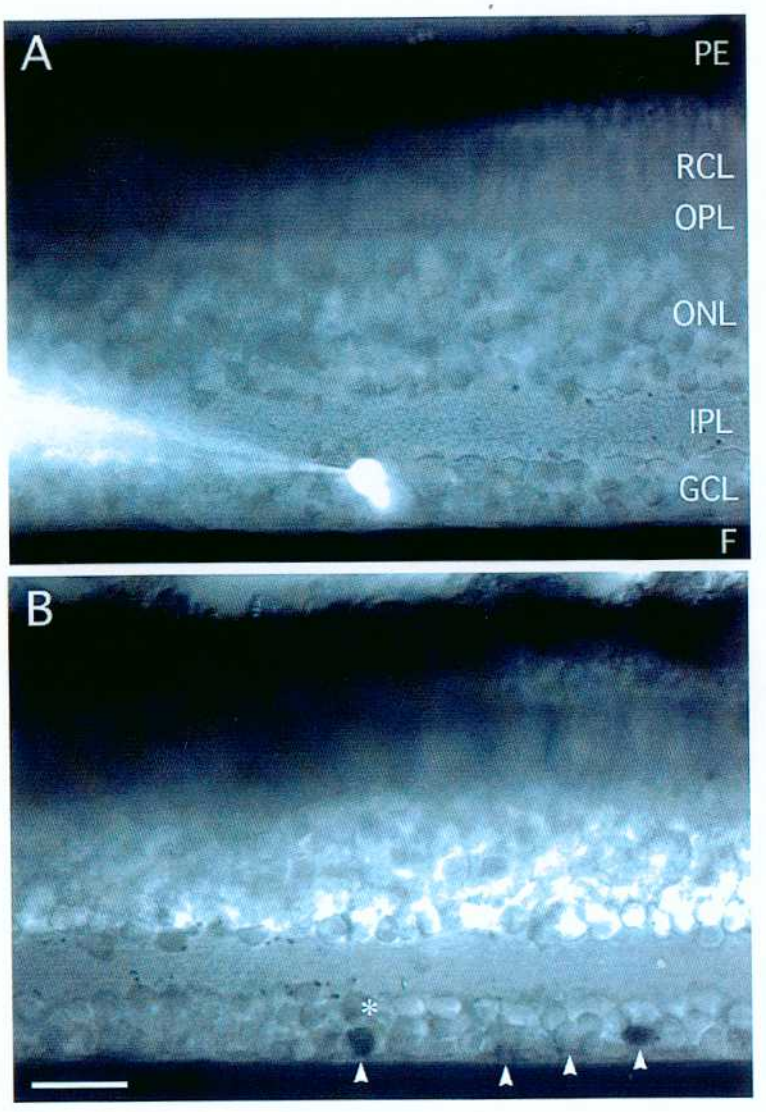
A
PE
RCL
OPL
ONL
IPL
GCL
F
B
*

Figure 16. Physiological and morphological development of ganglion cells during retinal regeneration.

Cells were depolarized from a holding potential of –100 mV to test voltages between –60 and 0 mV in 5 mV increments. Each step pulse of 8 ms duration was applied once every 1 s. Capacitive and leakage currents were reduced by the subtraction program. The cells were filled with LY from the recording electrode, after current recordings. **A:** The 'intermediate-II' regenerating retina. **B:** The 'intermediate-III' regenerating retina. **C:** The 'late' regenerating retina. **D:** The control retina. Abbreviations are the same as those in Fig. 8. Scale bar = 40 μm.

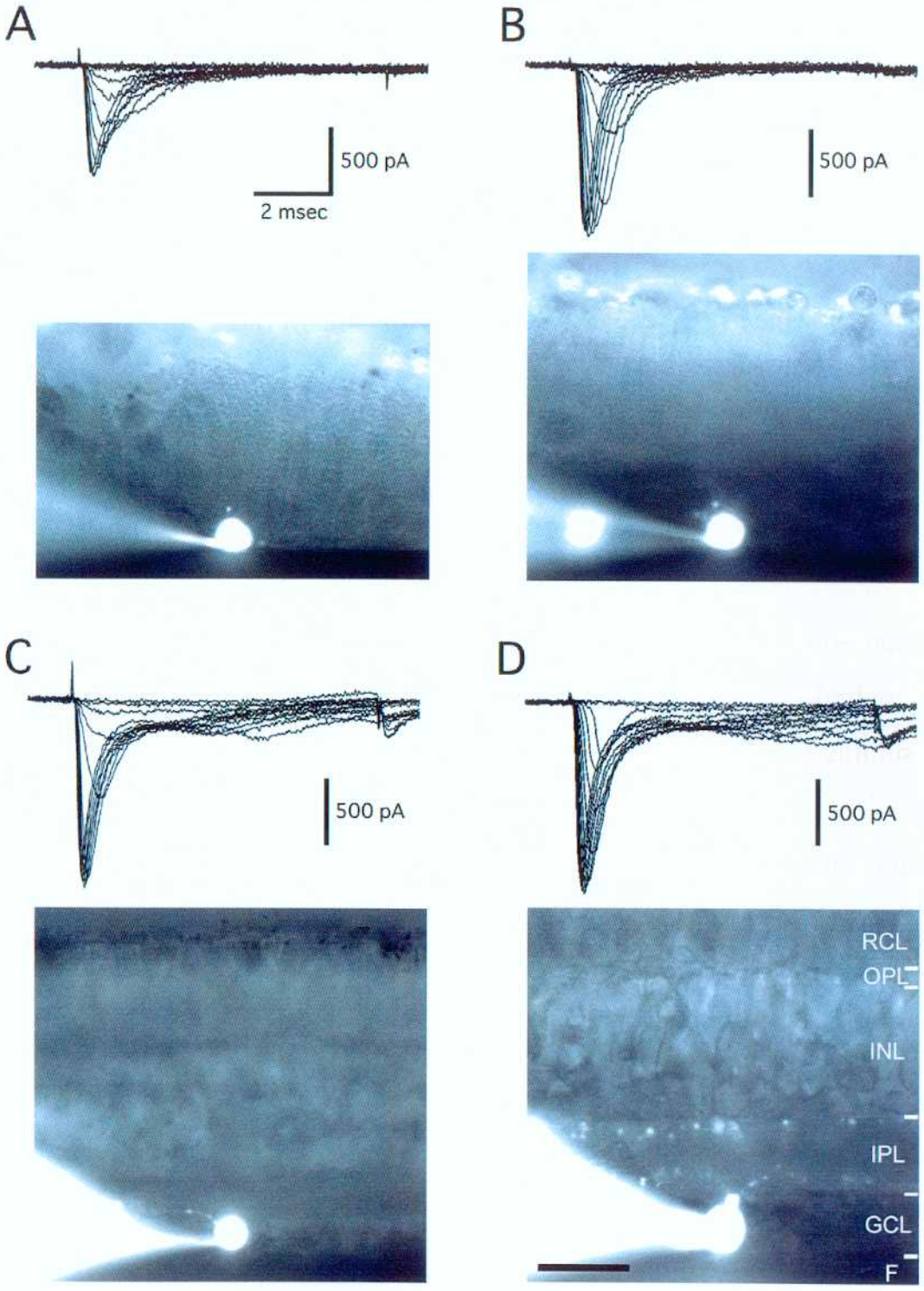
A
500 pA
2 msec
B
500 pA
C
500 pA
D
500 pA
RCL
OPL
INL
IPL
GCL
F

Figure 17. Appearance and maturation of voltage-gated Na^+ current in ganglion cells during retinal regeneration.

A: Appearance rate (%) of the Na^+ currents at different regeneration stages. Numbers in the parentheses indicate the number of cells tried. **B:** mean values (±SE) of the maximum Na^+ currents (●) and the activation threshold of the Na^+ current (▲) at different regeneration stages. Numbers in the parentheses indicate the number of cells examined. I. I, 'intermediate-I' regenerating retina; I. II, 'intermediate-II' regenerating retina; I. III, 'intermediate-III' regenerating retina; Late, 'late' regenerating retina; Control, adult retina.

A

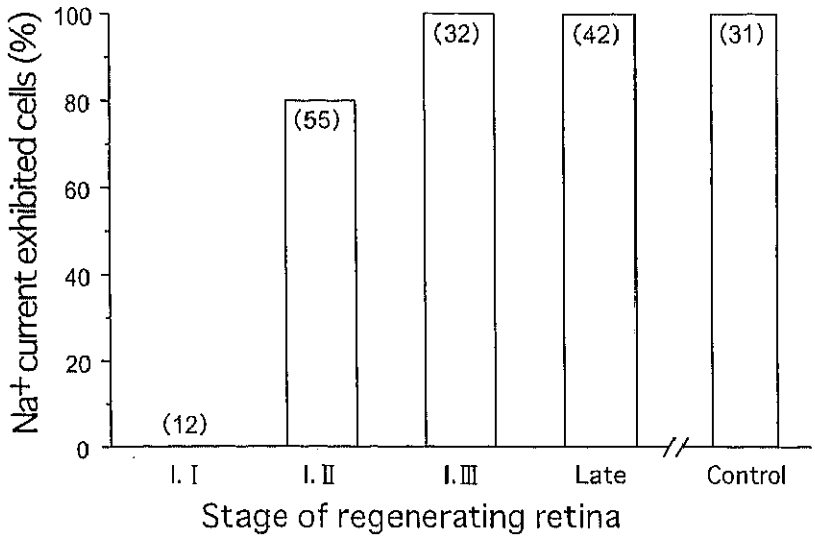
Na+ current exhibited cells (%)
100
80
60
40
20
0
(12)
(55)
(32)
(42)
(31)
I. I
I. II
I. III
Late
Control
Stage of regenerating retina

B

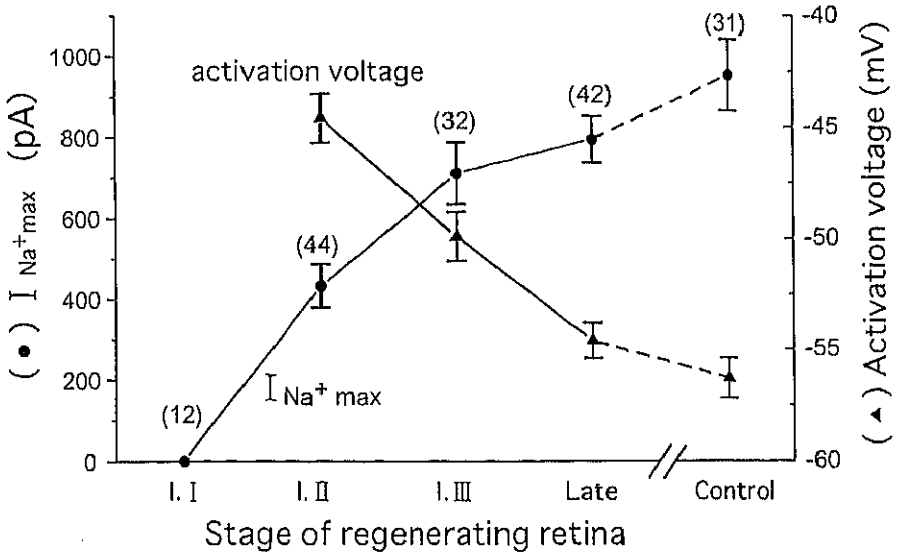
(•) I Na+max (pA)
1000
800
600
400
200
0
activation voltage
(12)
(44)
(32)
(42)
(31)
I Na+ max
-40
-45
-50
-55
-60
(▲) Activation voltage (mV)
I. I
I. II
I. III
Late
Control
Stage of regenerating retina

Figure 18. Schematic diagram showing 'Y-tube' drug application system. The control and drug-containing solutions were contained in 50 ml test tubes and connected with the inlet of the Y-tube through pinch valves. The test tubes were kept at a positive pressure with nitrogen, controlled by pico-pump. The outlet of the Y-tube was led to a drainage bottle through an electromagnetic valve. The drainage bottle was kept at a negative pressure by air pump. The tip of the Y-tube (100 μm i.d. and about 20 mm in length) was placed 200-300 μm away from the cell being recorded from. Whole-cell patch-clamp recording and perfusion of external solution were performed in the same way as in Fig. 5F.

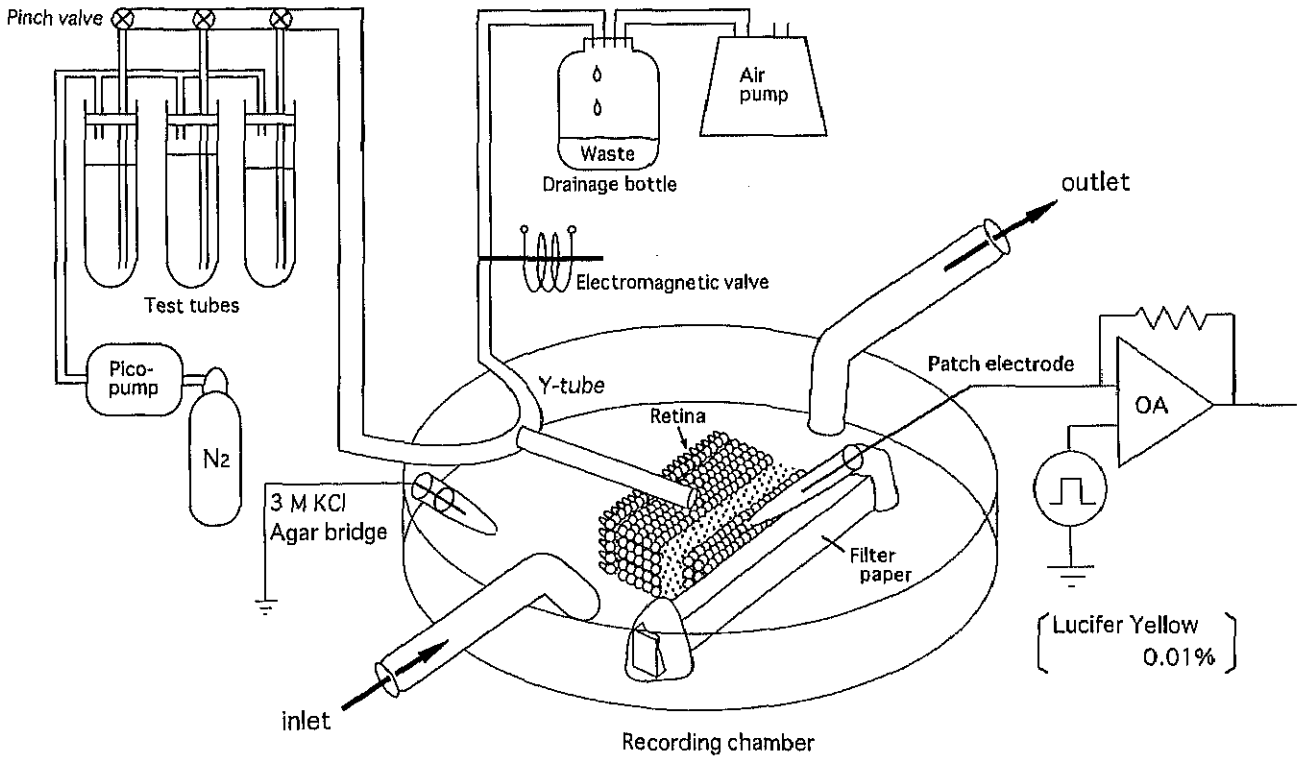
Pinch valve
Test tubes
Pico-
pump
N2
3 M KCl
Agar bridge
Waste
Drainage bottle
Air
pump
Electromagnetic valve
outlet
Y-tube
Retina
Patch electrode
OA
Filter
paper
Lucifer Yellow
0.01%
inlet
Recording chamber

Figure 19. Whole-cell currents elicited in ganglion cells in control retina by excitatory amino acid analogs and inhibitory amino acids.

Drugs were applied by the 'Y-tube' system. Cells were stained by LY and photographed under a combination of epifluorescent and incandescent lights (top panels). Both cells had dendritic processes that were distributed at both proximal and distal parts of the IPL. **A:** Responses to 100 μM AMPA (first trace) and 250 μM NMDA (second trace) at a holding potential of –80 mV. AMPA- and NMDA-induced currents were recorded in bath solution B and D, respectively. **B:** Responses to 30 μM GABA (first trace) and 30 μM glycine (Gly, second trace) at a holding potential of 0 mV. GABA- and glycine-induced currents were recorded in bath solution F. Drug-induced currents were recorded while suppressing synaptic transmission with $CoCl_2$ except NMDA-induced currents. V_H, holding potential. Other abbreviations are the same as those in Fig. 8. Scale bars = 30 μm.

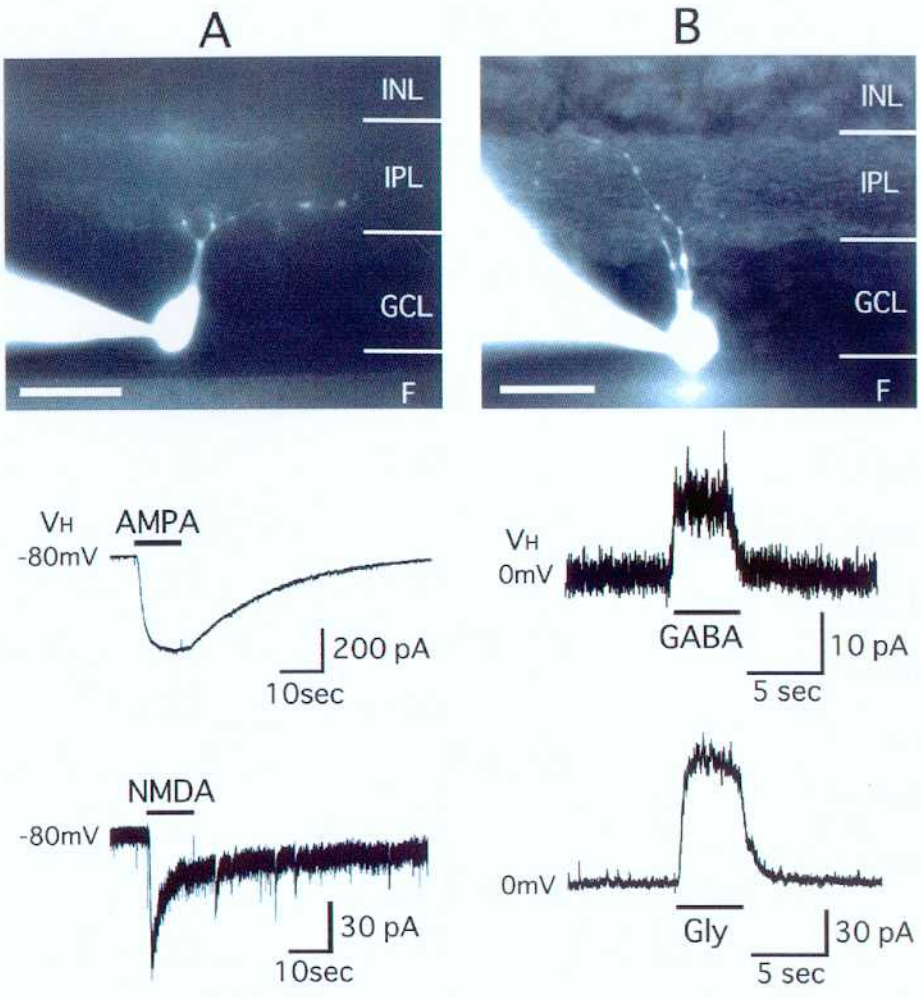
A
B
INL
IPL
GCL
F
INL
IPL
GCL
F
VH
-80mV
AMPA
200 pA
10sec
VH
0mV
GABA
10 pA
5 sec
NMDA
-80mV
30 pA
10sec
0mV
Gly
30 pA
5 sec

Figure 20. Current-voltage (I-V) relationships of excitatory amino acid analogs and inhibitory amino acids-induced currents in ganglion cells in control retina.

A: I-V curves for responses induced by 100 μM AMPA in solution B and 250 μM NMDA in solution D. Reversal potentials for AMPA (arrow) and NMDA (arrowhead) were –10 mV and –8 mV, respectively. **B:** I-V curves for responses induced by 100 μM GABA and 100 μM glycine in both solution F. Reversal potentials for GABA (arrow) and glycine (arrowhead) were –79 mV and –75 mV, respectively. Other recording conditions are the same as those in Fig. 19.

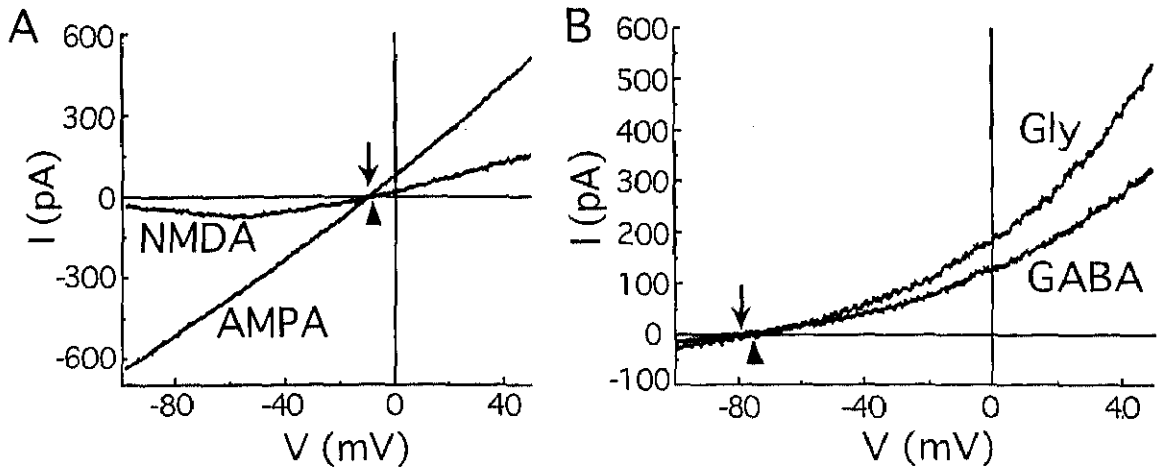
A
600
300
0
-300
-600
I (pA)
NMDA
AMPA
-80
-40
0
40
V (mV)
B
600
500
400
300
200
100
0
-100
I (pA)
Gly
GABA
-80
-40
0
40
V (mV)

Figure 21. Appearance of voltage- and ligand-gated ion currents in the 'intermediate-II' regenerating retina.

Examples of responses of two representative premature ganglion cells and morphology are shown. Cells were stained by LY and photographed under a combination of epifluorescent and incandescent lights (top panels). Both cells (**A** and **B**) had a rounded cell body and were exhibited voltage-gated Na^+ currents. Voltage-gated Na^+ currents were recorded in solution A (first traces). Cells were depolarized from a holding potential of –100 mV to test voltages between –60 and +25 mV in 5 mV increments. AMPA and NMDA responses were examined at a holding potential of –80 mV, and GABA and glycine responses were examined at a holding potential of 0 mV. AMPA- and NMDA-induced currents were recorded in bath solution B and D, respectively. GABA- and glycine-induced currents were recorded in bath solution F. Drug-induced currents were recorded under suppression of synaptic transmission by $CoCl_2$ except NMDA-induced currents. **A:** The cell did not respond to all drugs (second to fifth traces). **B:** The cell had an axon-like process (top panel, arrowhead) and responded to 100 μM AMPA, 30 μM GABA and 30 μM glycine, but not to 250 μM NMDA. All drugs were applied by the 'Y-tube' system. F, filter paper. Scale bars = 30 μm.

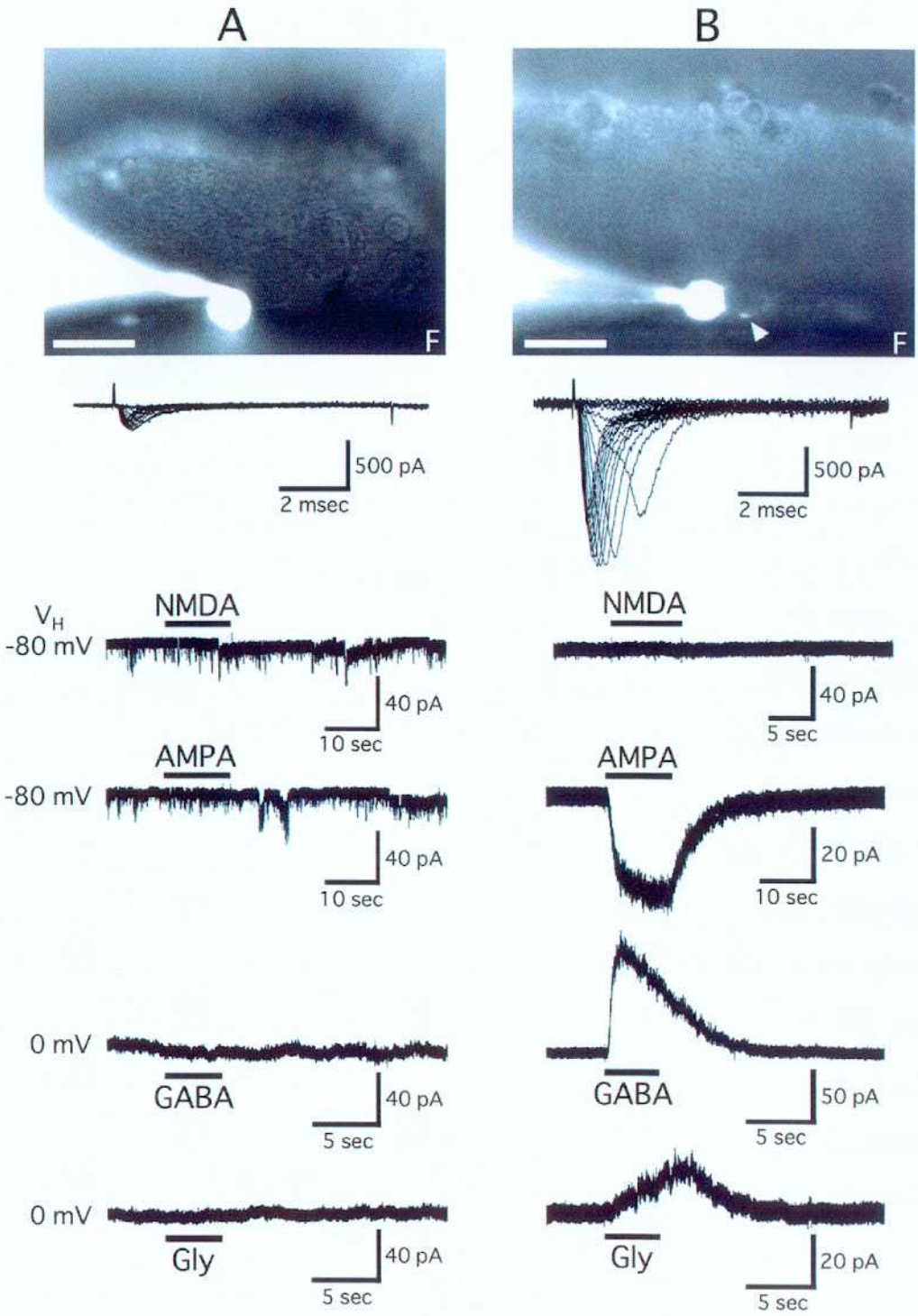
A
B
F
F
500 pA
2 msec
500 pA
2 msec
V_H
-80 mV
NMDA
40 pA
10 sec
NMDA
40 pA
5 sec
AMPA
-80 mV
40 pA
10 sec
AMPA
20 pA
10 sec
0 mV
GABA
40 pA
5 sec
GABA
50 pA
5 sec
0 mV
Gly
40 pA
5 sec
Gly
20 pA
5 sec

Figure 22. Responses of ganglion cells to excitatory amino acid analogs and inhibitory amino acids in the 'intermediate-III' (**A**) and 'late' (**B**) regenerating retina.

A: The cell had an axon-like process (top panel, arrowhead) and dendritic process (arrow) at the presumptive IPL, and exhibited the response not only to 100 μM AMPA, 100 μM GABA and 100 μM glycine (second to fifth traces) but also 250 μM NMDA (first trace). **B:** The cell had dendritic processes (arrow) at distal level of the IPL and could respond to all drugs (first to fourth traces). Other recording conditions and abbreviations are the same as those in Fig. 19. Scale bars = 40 μm.

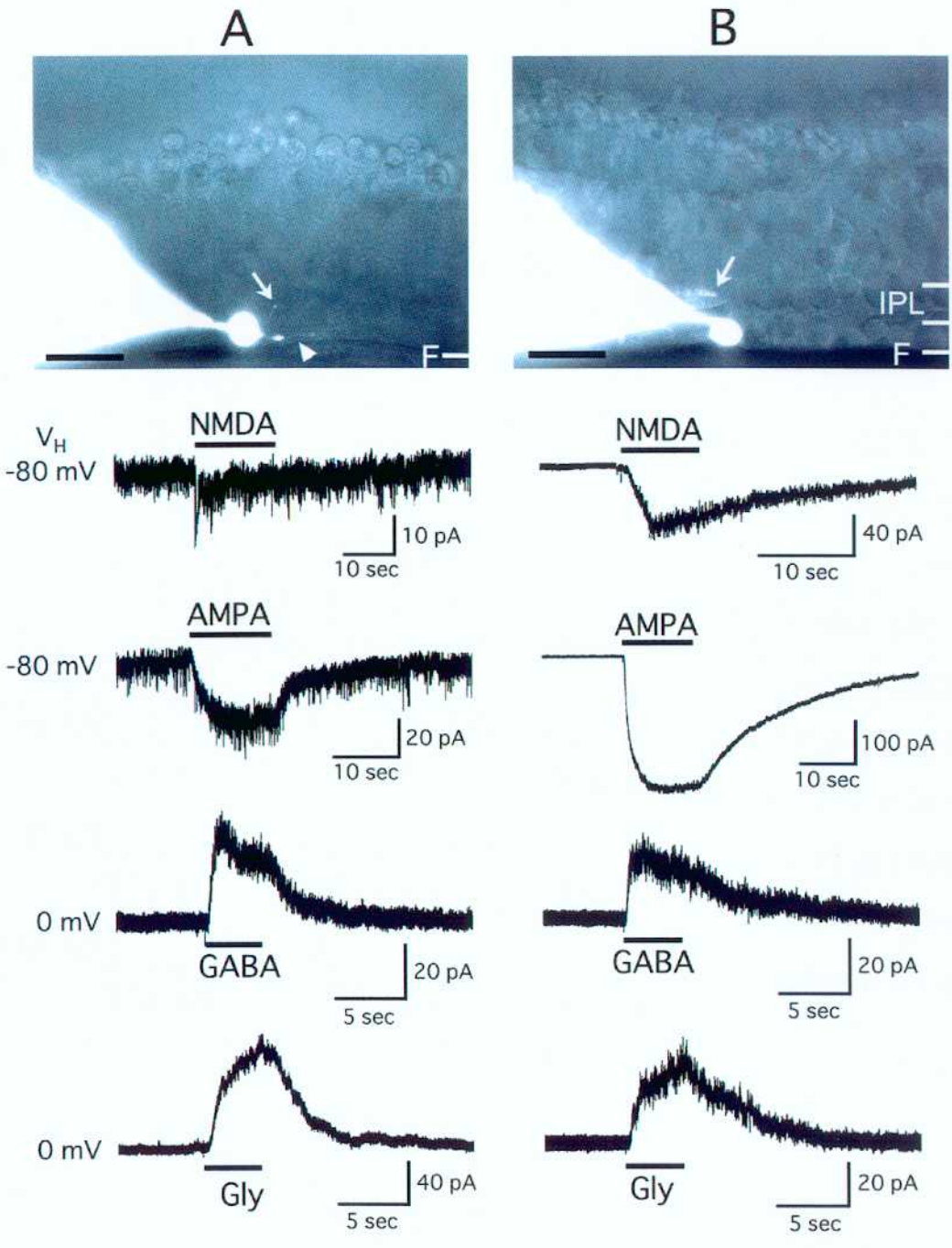
A
B
IPL
F
F
V_H
-80 mV
NMDA
10 pA
10 sec
NMDA
40 pA
10 sec
AMPA
-80 mV
20 pA
10 sec
AMPA
100 pA
10 sec
0 mV
GABA
20 pA
5 sec
GABA
20 pA
5 sec
0 mV
Gly
40 pA
5 sec
Gly
20 pA
5 sec

Figure 23. Appearance rate (%) of the drug-sensitive ganglion cells (bar graph) and mean amplitude (±SE) of the drug-induced currents (line graph) during retinal regeneration.

Other abbreviations are the same as those in Fig. 17. Numbers in the parentheses indicate the number of cells tried.

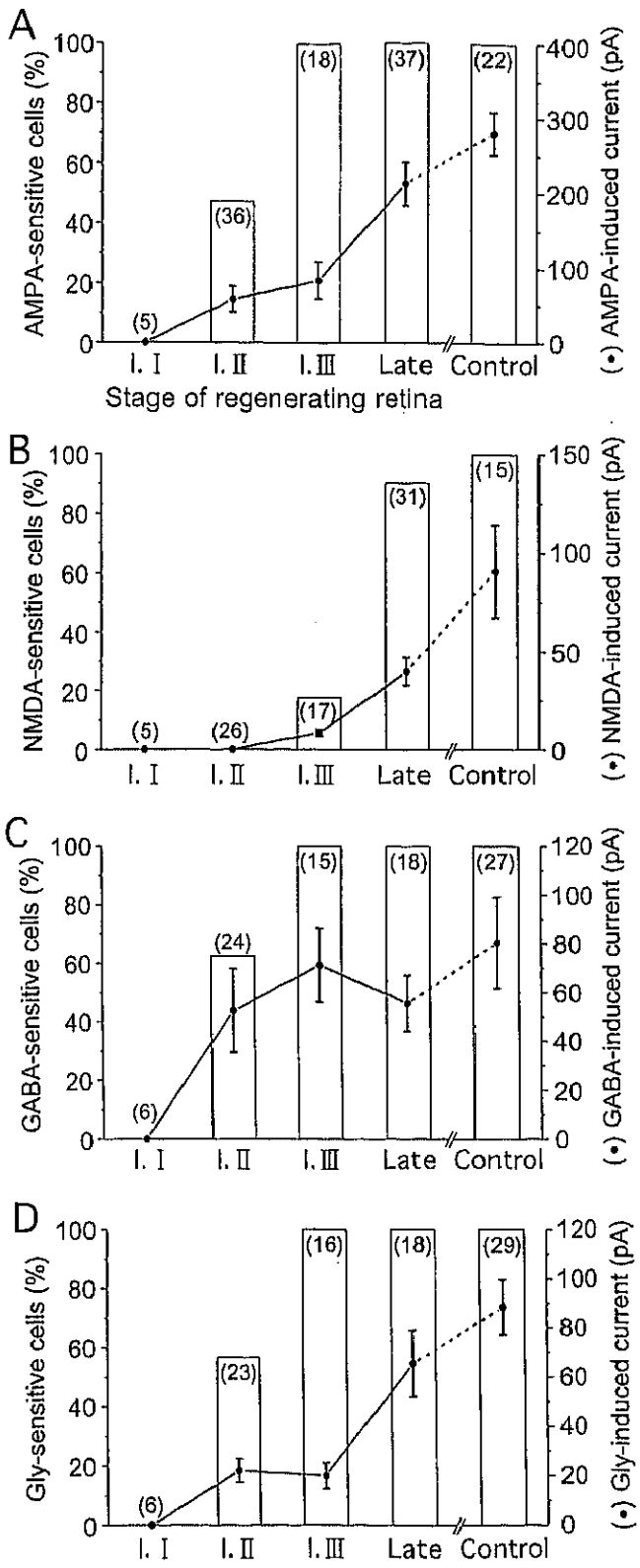
A
AMPA-sensitive cells (%)
(•) AMPA-induced current (pA)
(5)
(36)
(18)
(37)
(22)
I. I
I. II
I. III
Late
Control
Stage of regenerating retina
B
NMDA-sensitive cells (%)
(•) NMDA-induced current (pA)
(5)
(26)
(17)
(31)
(15)
C
GABA-sensitive cells (%)
(•) GABA-induced current (pA)
(6)
(24)
(15)
(18)
(27)
D
Gly-sensitive cells (%)
(•) Gly-induced current (pA)
(6)
(23)
(16)
(18)
(29)

Figure 24. Current-voltage (I-V) relationships of AMPA-, NMDA-, GABA- and Gly-induced currents in ganglion cells during retinal regeneration.

A: I-V curve for the response of a premature ganglion cell induced by 100 μM AMPA in the 'intermediate-II' regenerating retina. Reversal potential of the current was –7 mV. **C:** I-V curve of a ganglion cell induced by 250 μM NMDA in the 'late' regenerating retina. Reversal potential of the current was –5 mV. **E:** I-V curves for responses of a premature ganglion cell induced by 30 μM GABA and 100 μM glycine in the 'intermediate-II' regenerating retina. Reversal potentials for GABA and glycine were –69 mV and –67 mV, respectively. **B, D:** Comparison of the mean I-V relationship (±SE) in the regenerating ganglion cells with that of mature ganglion cells. Current responses for each cell were normalized to the response obtained at +40 mV. **B:** The normalized average I-V curves (n=5) for AMPA. **D:** The normalized average I-V curves (n=10) for NMDA. Records obtained from premature ganglion cells are indicated by the open circles (○), and those obtained from mature ganglion cells (**B**, n=12; **D**, n=7) are indicated by the filled circles (●). n, number of cells examined. Other recording conditions are the same as those in Fig. 19.

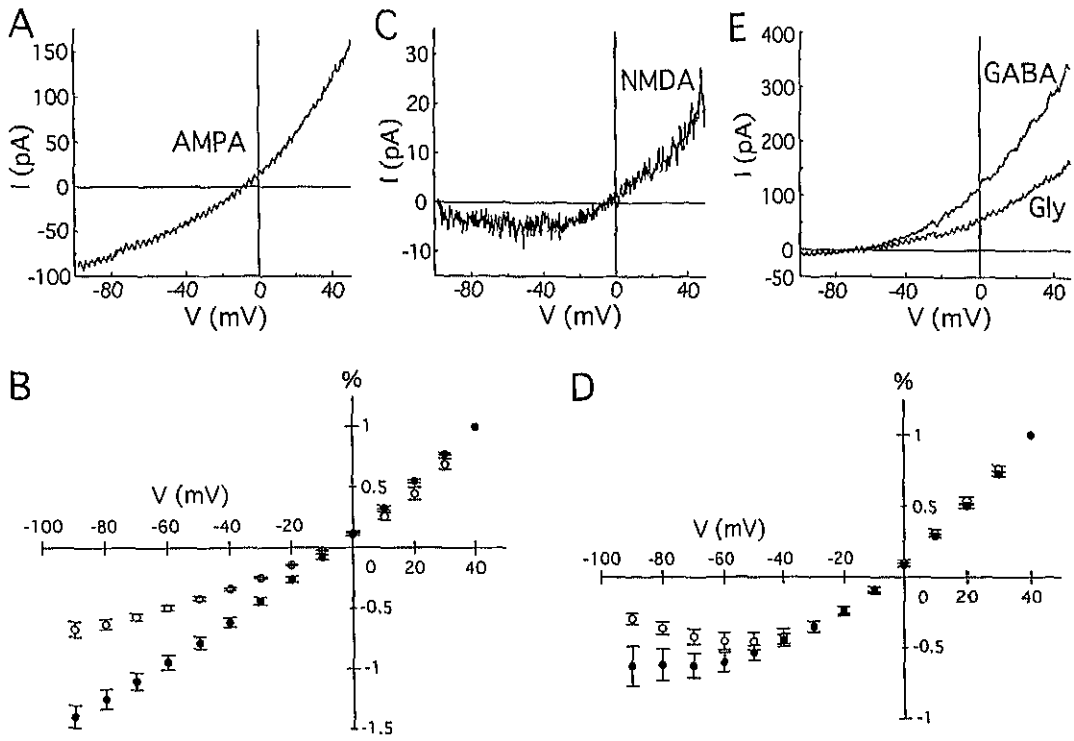
A
AMPA
I (pA)
V (mV)
C
NMDA
I (pA)
V (mV)
E
GABA
Gly
I (pA)
V (mV)
B
%
V (mV)
D
%
V (mV)

Figure 25. Effects of amino acid receptor antagonists on ganglion cells in regenerating retinas.

Holding potential was –80 mV for AMPA(A) and NMDA(B), and 0 mV for GABA(C) and glycine (D). CNQX and DL-AP7 were applied by the bath application system (opened bar). Bicuculline and strychnine were co-applied with GABA and glycine by the 'Y-tube' system (closed bar), respectively. **A:** CNQX (50 μM) completely suppressed AMPA (100 μM)-induced current (middle) of a premature ganglion cell in the 'intermediate-II' regenerating retina. The response amplitude recovered to 62% amplitude of the control (left) after 10 min washing (right). **B:** DL-AP7 (100 μM) reduced NMDA (250 μM)-induced current (middle) of a ganglion cell in the 'late' regenerating retina. The response amplitude recovered to 37% amplitude of the control (left) after 9 min washing (right). **C:** Bicuculline (20 μM) almost completely suppressed the GABA (30 μM)-induced current (middle) of a premature ganglion cell in the 'intermediate-II' regenerating retina. The response amplitude recovered to 76% amplitude of the control (left) after 3 min washing (right). **D:** Strychnine (2 μM) almost completely suppressed the glycine (30 μM)-induced current (middle) of a premature ganglion cell in the 'intermediate-II' regenerating retina. The response amplitude recovered to 77% amplitude of the control (left) after 4 min washing (right). Other recording conditions are the same as those in Fig. 19.

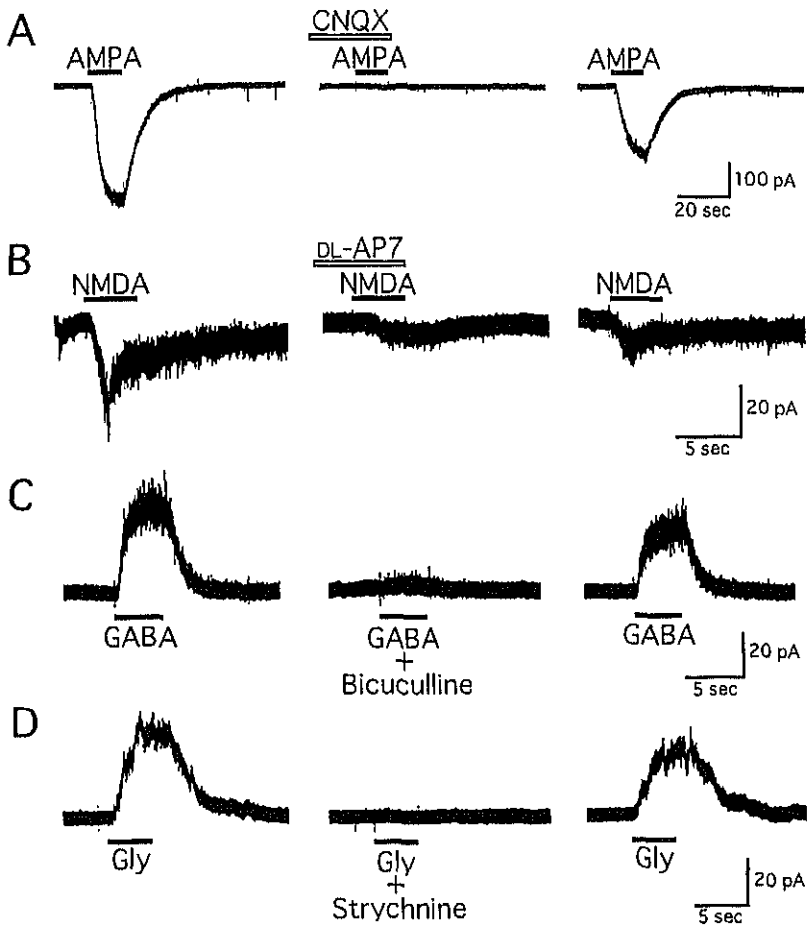
A
AMPA
CNQX
AMPA
AMPA
100 pA
20 sec
B
NMDA
DL-AP7
NMDA
NMDA
20 pA
5 sec
C
GABA
GABA
+
Bicuculline
GABA
20 pA
5 sec
D
Gly
Gly
+
Strychnine
Gly
20 pA
5 sec

Figure 26. Morphological and functional characteristics of regenerating retinas at different stages (**A**) and the correlation between cell-to-cell communication and neurogenesis (**B**).

A: Schematic diagram illustrating the appearance and disappearance of gap junctions, and the appearance and maintenance of Na^+ channels and excitatory and inhibitory amino acid receptors. The upper halve of the diagram is the same as B in Fig. 8. Abbreviations are the same as those in Fig. 8.

B: Schematic diagram showing two possible cell-to-cell communications, the Delta-Notch lateral-inhibitory signaling pathway and gap junctions, and their correlation with neurogenesis and neuronal differentiation. N, nucleus.

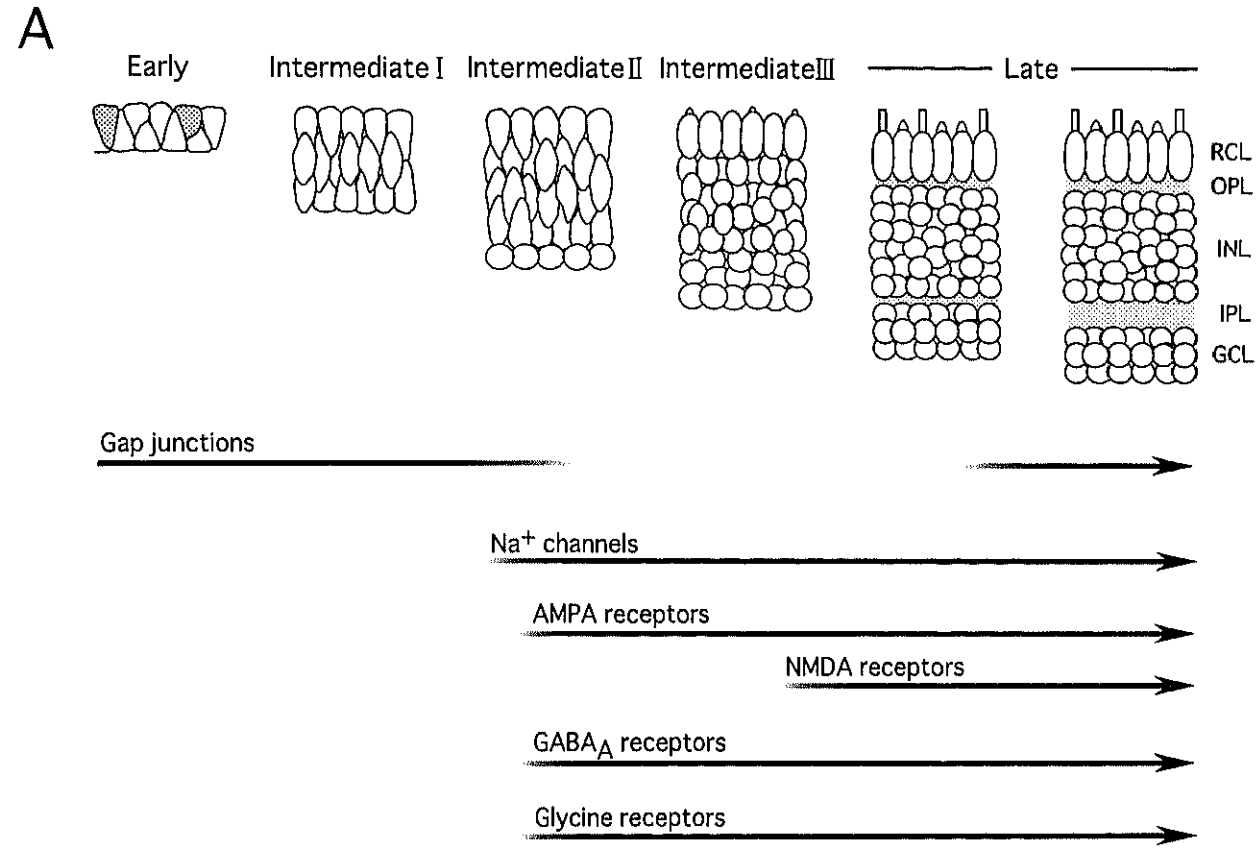
A
Early
Intermediate I
Intermediate II
Intermediate III
Late
RCL
OPL
INL
IPL
GCL
Gap junctions
Na+ channels
AMPA receptors
NMDA receptors
GABAA receptors
Glycine receptors

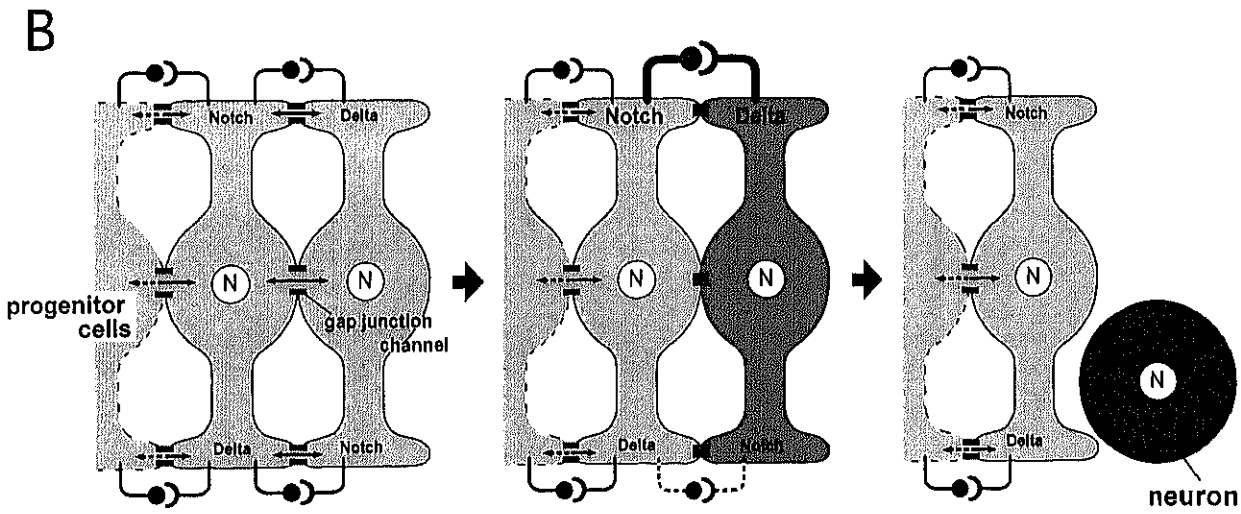
B
Notch
Delta
N
progenitor cells
gap junction channel
neuron